

Discrimination of product isomers in the photodissociation of propyne and allene at 193 nm

Weizhong Sun, Keiichi Yokoyama,^{a)} Jason C. Robinson, Arthur G. Suits, and Daniel M. Neumark

Department of Chemistry, California, and Chemical Sciences Division, Lawrence Berkeley National Laboratory, University of California, Berkeley, California 94720

(Received 8 September 1998; accepted 20 November 1998)

The photodissociation dynamics of propyne and allene are investigated in two molecular beam/photodissociation instruments, one using electron impact ionization and the other using tunable vacuum ultraviolet (VUV) light to photoionize the photoproducts. The primary dissociation channels for both reactants are C_3H_3+H and $C_3H_2+H_2$. Measurement of the photoionization efficiency curves on the VUV instrument shows that the C_3H_3 product from propyne is the propynyl (CH_3CC) radical, whereas the C_3H_3 product from allene is the propargyl (CH_2CCH) radical. The dominant C_3H_2 product from both reactants is the propadienylidene (H_2CCC) radical. We also observe a small amount of secondary C_3H_2 product from photodissociation of the C_3H_3 radicals in both cases. © 1999 American Institute of Physics. [S0021-9606(99)02008-5]

INTRODUCTION

As the field of reaction dynamics evolves toward the study of more complex chemistry, it becomes necessary to develop new methods for probing the products of bimolecular and unimolecular reactions. The photodissociation of hydrocarbon molecules exemplifies the challenges one faces. Cleavage of the various inequivalent C–H bonds will result in chemically distinct isomers with the same mass, thereby complicating the identification of the primary photodissociation products. The well-established technique of molecular beam photodissociation with product detection by electron impact ionization cannot, in general, distinguish among isomers. While laser-based methods such as laser-induced fluorescence or resonant multiphoton ionization can in principle do better, this requires a fuller understanding of the electronic spectroscopy of polyatomic hydrocarbon radicals than is often available. On the other hand, isomers of hydrocarbon radicals often have different ionization potentials. This is exploited in the work presented here, where tunable vacuum ultraviolet (VUV) radiation from the Berkeley Advanced Light Source is used to ionize and therefore identify the products of the photodissociation of allene and propyne.

Propyne (CH_3CCH) and allene (H_2CCCH_2) both have chemical formula C_3H_4 . While C–H bond fission in allene can lead only to propargyl (CH_2CCH) radical production, propyne can yield either the propargyl or propynyl (CH_3CC) radical. The latter channel is energetically disfavored by 41 kcal/mole.^{1,2} In 1966, Ramsay and Thistlethwaite found that the flash photolysis of allene and propyne resulted in the same species which was assigned as propargyl radical.³ Two more recent isotopic studies^{4,5} suggest, in contrast, that pho-

tolysis of propyne at 193 nm breaks the acetylenic C–H bond exclusively. The two observations can be reconciled if any CH_3CC produced in the flash photolysis experiment rearranges to form the lower energy propargyl isomer on the time scale of the experiment (25 μs).

The work presented here clearly shows the H-atom loss channel in the photodissociation of propyne at 193 nm results corresponds almost exclusively to propynyl production. We also investigate the other primary and secondary photodissociation channels of allene and propyne at 193 nm. The other major primary channel is H_2 loss to produce C_3H_2 . We identify this as the propadienylidene (H_2CCC) isomer, and find that this channel is considerably more important than was concluded in a previous photodissociation study of allene.⁶ We also find that C_3H_2 is produced by a secondary process, namely the photodissociation of C_3H_3 radicals.

EXPERIMENT

The photodissociation dynamics of the two reactants are studied using molecular beam photofragment translational spectroscopy.^{7,8} Two crossed molecular beam instruments, differing primarily in the detector ionization scheme, were used in this study. The electron impact (EI) apparatus is a standard crossed beam instrument⁷ in which scattered products are ionized via electron impact. In these experiments, a supersonic pulsed molecular beam of reactant seeded in neon is crossed at 90° with the output of an (unpolarized) excimer laser operating on the ArF transition (193.3 nm). The laser pulse energy used in these experiments varied from 50–100 mJ and was focused to a 2×3 mm² spot. The photoproducts that recoil out of the molecular beam at a particular scattering angle are detected by a triply-differentially-pumped rotating mass spectrometer, in which they are ionized by electron impact and mass-selected with a quadrupole mass

^{a)}Permanent address: Japan Atomic Energy Research Institute, Tokai-mura, Ibruraki, 319-11 Japan.

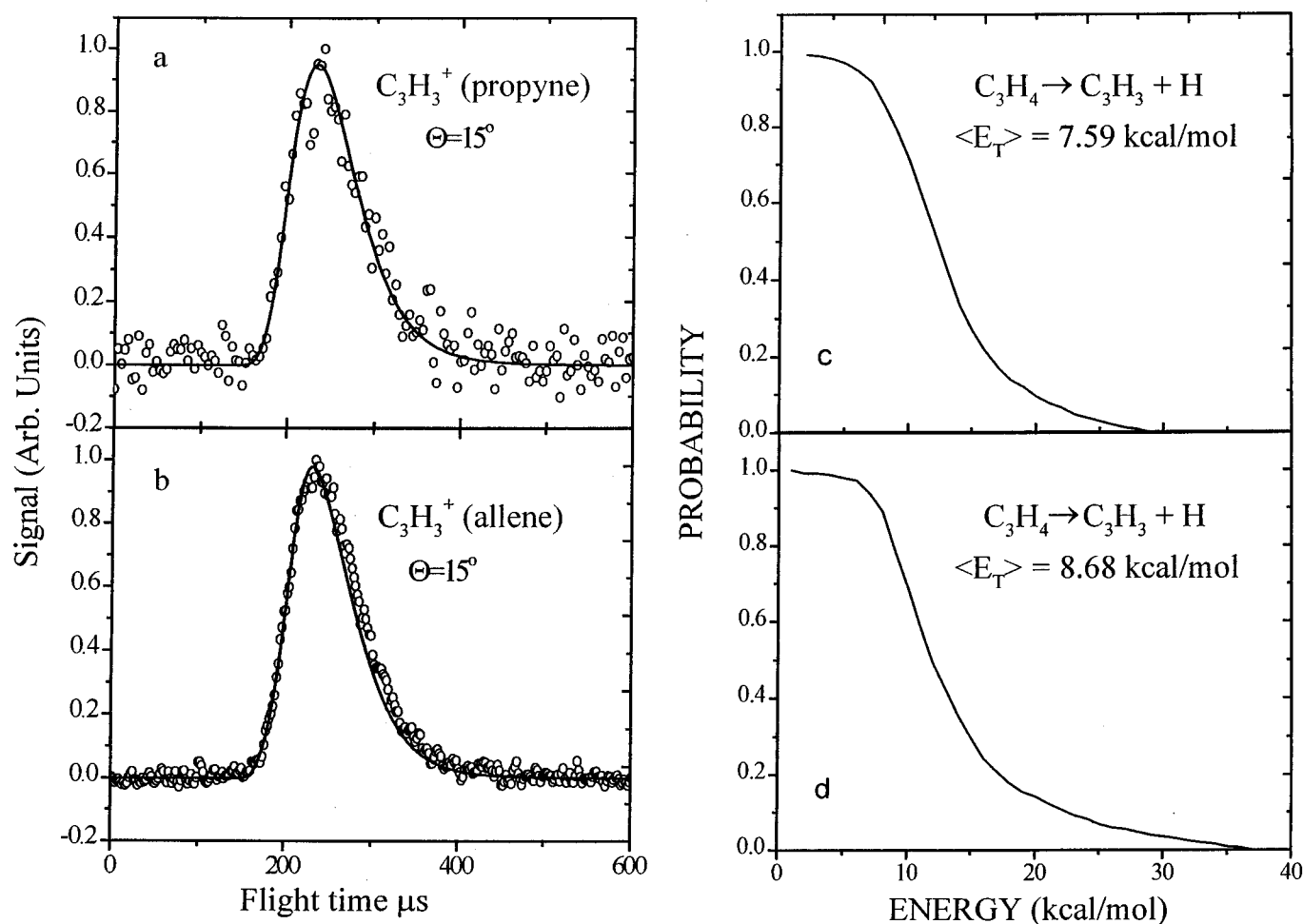


FIG. 1. Time-of-flight (TOF) spectra for $C_3H_3^+$ at $\Theta = 15^\circ$ from 193 nm photodissociation of (a) propyne and (b) allene on the EI instrument. Solid curves in (a) and (b) are from forward convolution of the center-of-mass translational energy distributions $P(E_T)$ shown in (c) and (d) for propyne and allene dissociation, respectively. The "tail" in Fig. 1(c) beyond $E_T = 18$ kcal/mol is from allene impurity in the propyne beam.

spectrometer. Laboratory time-of-flight (TOF) distributions, measured with respect to the photolysis pulse, are taken at a series of scattering angles. These laboratory-frame distributions are fit using a forward-convolution technique, yielding the translational energy distribution $P(E_T)$ in the center-of-mass (c.m.) reference frame.⁹

The second instrument (the PI instrument) is a crossed beams apparatus connected to the Chemical Dynamics Beamline at the Berkeley Advanced Light Source (ALS). Although similar in many ways to the EI apparatus, the source rotates rather than the detector, and the scattered photoproducts are photoionized by tunable VUV radiation.¹⁰ The VUV radiation is generated in the U10 undulator of the ALS, and is injected directly into the PI instrument without passing through a monochromator. This VUV light, which has a bandwidth of about 2%, can be tuned by varying the undulator gap. This allows us to measure photoionization efficiency (PIE) curves for photoproducts at various scattering angles, yielding the ionization potential for the scattered photoproduct. In addition, laboratory TOF distributions were

measured for allene (but not propyne) photodissociation using VUV ionization at selected photon energies. In all PI experiments a continuous molecular beam was used. The reactant gases were seeded in He for the PIE measurements and Ne for the TOF measurements.

RESULTS AND DISCUSSION

TOF spectra on both instruments were measured at several laboratory angles between 7° and 25° for $m/e = 39$, 38, 37, and 36, corresponding to the ions $C_3H_3^+$, $C_3H_2^+$, C_3H^+ , and C_3^+ . Allene product TOF spectra were measured on the EI and PI instruments, whereas TOF measurements for propyne photodissociation were measured on the EI instrument only. Only the $m/e = 39$ and 38 results are discussed in this paper.

Figure 1 shows TOF spectra at laboratory angle $\Theta = 15^\circ$ for mass 39 from the photodissociation of propyne [Fig. 1(a)] and allene [Fig. 1(b)] on the EI instrument. These TOF spectra as well as those taken at several other scattering

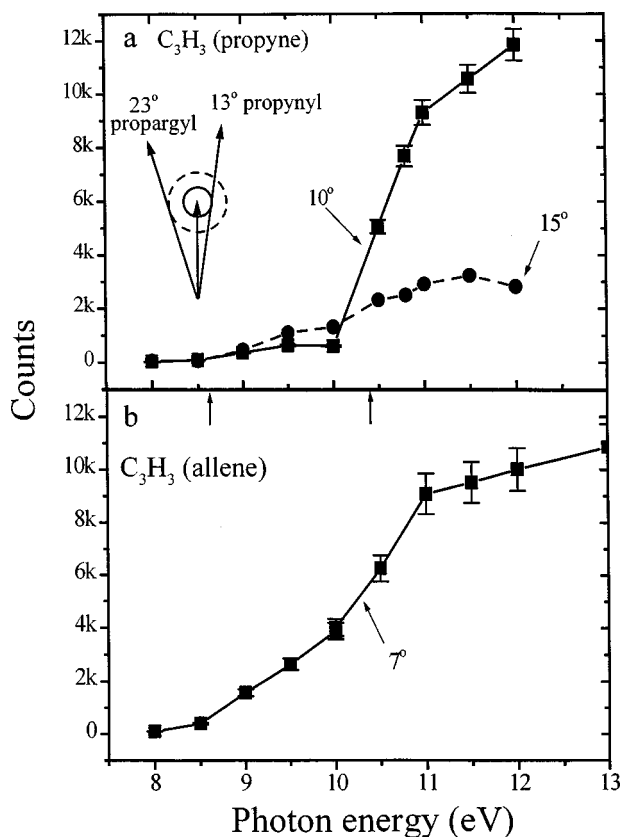


FIG. 2. Photoionization efficiency curves of C_3H_3 product at $\Theta = 10^\circ$ and 15° from photodissociation of (a) propyne and (b) from allene photodissociation at $\Theta = 7^\circ$. Inset in (a) shows Newton diagram for propyne photodissociation, with Θ_{\max} shown for propynyl and propargyl products. Arrows on energy axis indicate ionization potentials for propargyl (8.67 eV) and propynyl (10.8 eV) from Table I.

angles were fit by forward convolution⁹ to the CM translational energy distributions shown in Figs. 1(c) and 1(d) for propyne and allene, respectively. The two distributions are quite similar, with a slightly higher average translational energy $\langle E_T \rangle$ for the allene photoproduct.

However, the photoionization efficiency curves for the C_3H_3 photoproduct from propyne and allene in Figs. 2(a) and 2(b), respectively, are very different. These were obtained on the PI instrument at the laboratory angles indicated. At $\Theta = 10^\circ$, the C_3H_3 product from propyne photodissociation shows an ionization threshold around 10.25 eV, whereas that from allene photodissociation (at $\Theta = 7^\circ$) shows a threshold around 8.5 eV. Experimental^{2,11-13} and theoretical¹⁴ ionization potentials and heats of formation of the various C_3H_3 (and C_3H_2) isomers are listed in Table I. Comparison with the data in Fig. 2 indicates that the C_3H_3 isomer from propyne dissociation is primarily the propynyl radical, and the C_3H_3 isomer from allene is the propargyl radical. This is confirmed by the PIE curve for C_3H_3 from propyne at $\Theta = 15^\circ$ [Fig. 2(a)], which lies outside the Newton circle for propynyl radical; under the conditions of this experiment, $\Theta_{\max} = 13^\circ$ for propynyl, as shown in the inset of Fig. 2(a). The threshold at 10.25 eV is gone, and what remains looks

TABLE I. Ionization potentials and heats formation of various C_3H_4 , C_3H_3 , and C_3H_2 isomers.

Formula	Isomer	IP (eV)	ΔH_f (kcal/mole)
C_3H_4	CH_3CCH	10.36 (Ref. 11)	45.8 ± 2.6 (Ref. 1)
	CH_2CCH_2	9.53 ± 0.03 (Ref. 11)	47.7 ± 3.4 (Ref. 1)
C_3H_3	CH_3CC	10.8 (Ref. 14)	122.4 ± 3 (Ref. 2)
	CH_2CCH	8.67 ± 0.02 (Ref. 12)	82.5 ± 3 (Ref. 2)
C_3H_2	H_2CCC	10.43 ± 0.02 (Ref. 13)	133.4 ± 2.5 (Ref. 1)
	$HCCCH$	8.7 (Ref. 13)	129.4 ± 8.4 (Ref. 1)
	$c-C_3H_2$	9.15 ± 0.03 (Ref. 13)	118.6 (Ref. 16)

very much like the curve in Fig. 2(b). In fact, given that propyne has 3% allene impurity, and that the dissociation cross section of allene is about 5 times larger than propyne at 193 nm,¹⁵ the signal in Fig. 2(a) at $\Theta = 15^\circ$ is almost entirely due to the allene impurity. Thus, within experimental error, it appears that all the C_3H_3 product from propyne is propynyl radical.

The dissociation energy of the acetylenic bond in propyne is 130 kcal/mol, whereas that for the methyl C–H bond is 89 kcal/mol.^{1,2,16} The 193 nm photolysis of propyne therefore results in cleavage of the stronger bond. This clear example of bond-selective chemistry shows that dissociation occurs on an electronically excited surface; cleavage of the acetylenic C–H bond presumably results from its proximity to the $C \equiv C$ bond where the initial excitation occurs via a $\pi^* \leftarrow \pi$ transition. Although the propynyl radical can in principle isomerize to the lower energy propargyl radical, our experiment indicates that this does not happen. A recent theoretical study predicts an isomerization barrier of 34.4 kcal/mol for this process,¹⁶ but since the photon energy at 193 nm is 148 kcal/mol, only 18 kcal/mol internal energy at most is available for propynyl product. The absence of isomerization is not surprising under these circumstances.

TOF spectra for mass 38 are shown in Fig. 3. Figures 3(a) and 3(b) show results from propyne and allene dissociation, respectively, on the EI instrument at 15° while Figs. 3(c) and 3(d) show results from allene dissociation at 15° on the PI instrument at two different photoionization energies, 12 and 10 eV. There are three contributions to the signal at mass 38: (a) dissociative ionization of C_3H_3 , (b) the primary photolysis channel $C_3H_4 + h\nu \rightarrow C_3H_2 + H_2$, and (c) the secondary photolysis channel $C_3H_3 + h\nu \rightarrow C_3H_2 + H$.

In the absence of the PI measurements, the contribution from dissociative ionization can be assessed from the TOF distributions in Fig. 1. Further clarification comes from a comparison of Figs. 3(b) and 3(c). There is considerably less signal from dissociative ionization of C_3H_3 in the PI data since the energetic threshold for this process is around 14 eV. (There is some contribution due to about 4% leakage of mass 39 ions through the mass filter plus a small amount of dissociative ionization from the high energy tail of the VUV

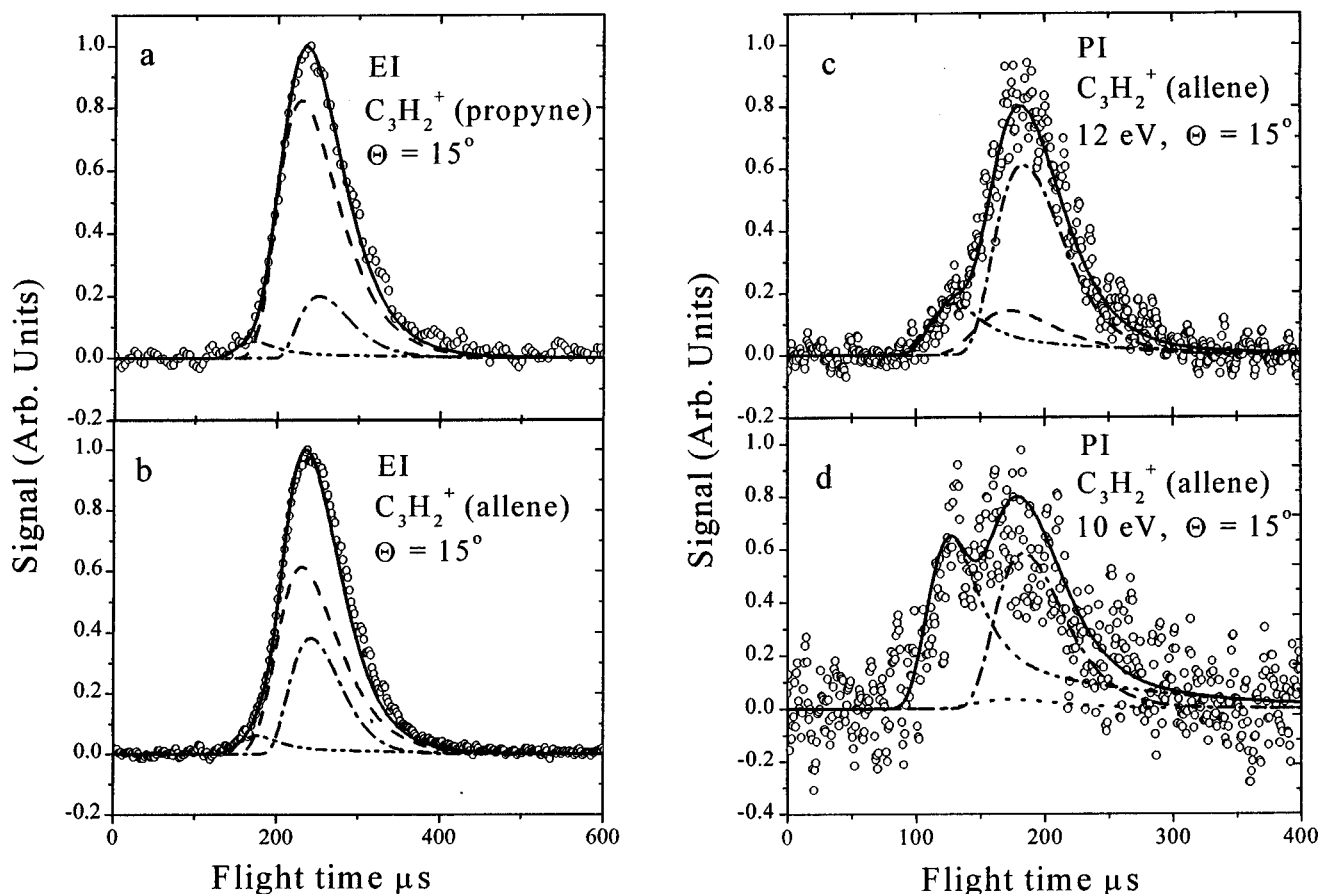


FIG. 3. TOF spectra of $C_3H_2^+$ from propyne and allene dissociation. Results from propyne and allene dissociation on EI instrument at $\Theta = 15^\circ$ are shown in (a) and (b), respectively. Results from allene at 15° on PI instrument at photon energies of 12 and 10 eV are shown in (c) and (d), respectively. Each plot shows experimental data (open circle) and contributions from dissociative ionization of C_3H_3 (dashed), primary $C_3H_2+H_2$ channel (dashed-dot), and secondary photolysis of C_3H_3 (dashed-dot-dot).

radiation.¹⁷) As a consequence, a fast shoulder due to secondary photolysis is apparent in Fig. 3(c) from 100–140 μ s. This shoulder can barely be seen in the EI data at $\Theta = 15^\circ$ [i.e., Figs. 3(a) and 3(b)] but becomes far more prominent at larger angles (not shown) for propyne and allene. By fitting the EI and (for allene) PI data at 12 eV at several laboratory angles, we constructed CM translational energy distributions for C_3H_2 from primary and secondary photolysis. These are shown in Figs. 4(a) and 4(c) for propyne and Figs. 4(b) and 4(d) for allene. The contributions from processes (a), (b), and (c) to each laboratory TOF spectrum are indicated in Fig. 3.

Data on the PI instrument at 10 eV were taken only at $\Theta = 15^\circ$ [Fig. 3(d)]. This data was not used in constructing the $P(E_T)$ distributions, due to its low signal-to-noise. Comparison with Fig. 3(c) shows that the relative intensity of the fast peak from secondary photolysis is significantly larger at 10 eV. This shows that the C_3H_2 product from secondary photolysis has a lower ionization potential than that from primary photolysis.

Photoionization efficiency curves for mass 38 at 10° from propyne and 15° from allene are shown in Figs. 5(a) and 5(b), respectively. Both curves show an abrupt onset at 10.5–11 eV. Comparison with the ionization potentials for

the C_3H_2 isomers¹³ listed in Table I shows that this threshold corresponds to the propadienylidene (H_2CCC) isomer, indicating this is the dominant mass 38 product regardless of reactant. This observation is of interest because H_2CCC is calculated to lie 8.7 kcal/mol above the cyclic C_3H_2 structure.¹⁶ Primary production of propadienylidene from allene presumably occurs via three-center elimination of H_2 . In propyne, a possible mechanism would be production of propargylene ($HCCCH$) by three-center elimination followed by isomerization to the lower energy H_2CCC structure.¹⁸ The above comparison of Figs. 3(c) and 3(d) indicates that much of the low energy tail below 10.5 eV corresponds to C_3H_2 produced by secondary photolysis. This signal could be due to the cyclic isomer or to highly vibrationally excited H_2CCC .

We now consider the $P(E_T)$ distributions from Fig. 4 in more detail. The translational energy release of the primary $C_3H_2+H_2$ channel is very small, having an average energy of only 1.56 kcal/mole for propyne dissociation and 2.49 kcal/mole for allene dissociation. This indicates that the products are highly internally excited, with about 61 kcal/mole of internal excitation.

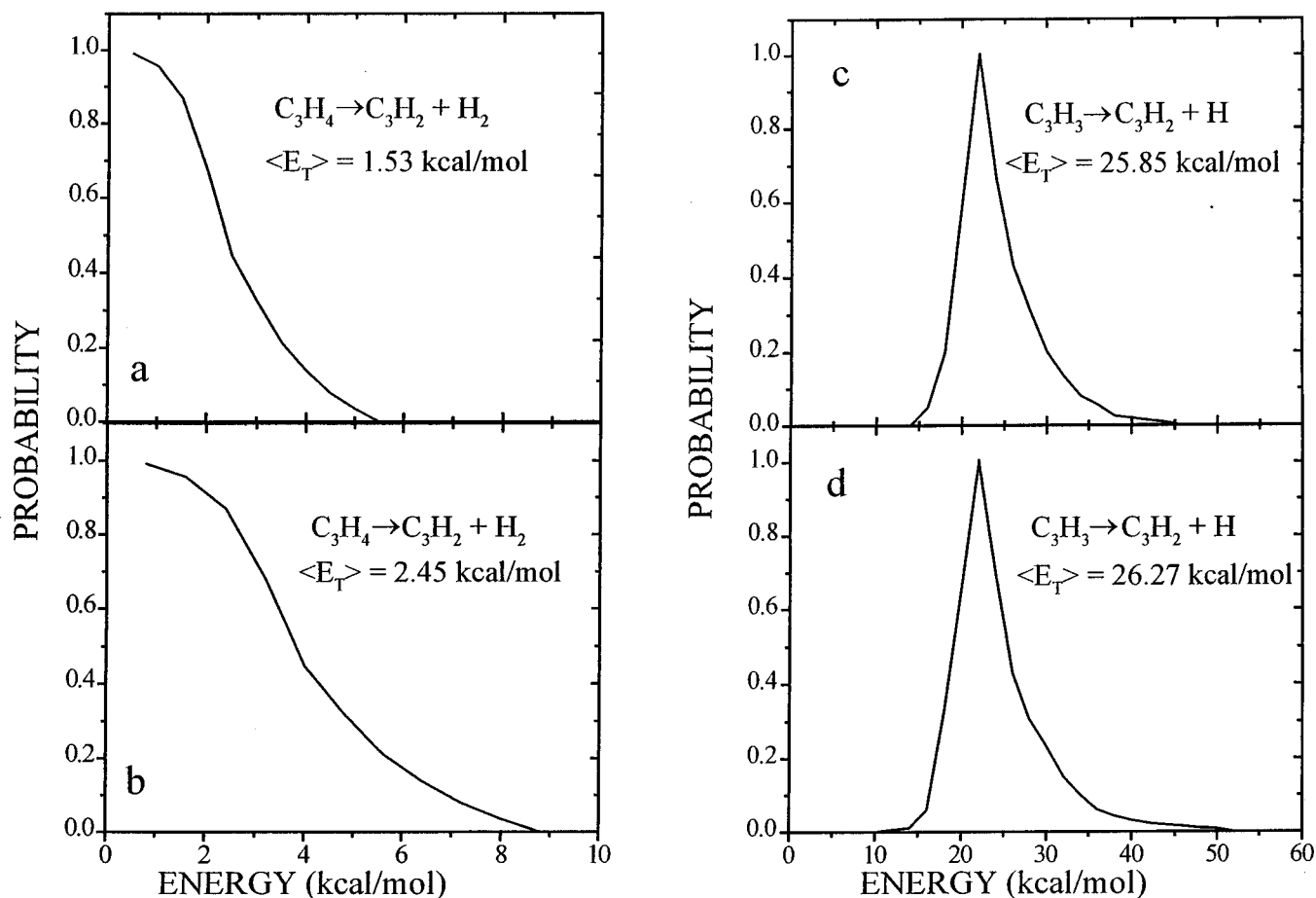


FIG. 4. $P(E_T)$ distributions of C_3H_2 from propyne and allene photodissociation. (a) and (c) are distributions for primary $C_3H_2+H_2$ and secondary C_3H_2+H channels, respectively, from propyne. (b) and (d) are analogous distributions from allene.

The $P(E_T)$ distributions for C_3H_2 produced by secondary photolysis both peak around 22 kcal/mol, and fall off sharply toward lower E_T . The low energy fall off is attributed to spontaneous dissociation of C_3H_2 radicals formed with internal energies above 84.0 kcal/mol, the calculated bond dissociation energy to form cyclic C_3H+H (the cyclic isomer is the most stable).^{16,19} From Table I, and using $\Delta H_f(H) = 52.1$ kcal/mol, the acetylenic C–H bond dissociation energy in propyne is 130.1 kcal/mol, and dissociation of propynyl to H_2CCC+H requires 61.7 kcal/mol. If the C_3H_3+H channel were formed with no translational energy, then the total energy available to the C_3H_2 product is 296 (i.e., two 193 nm photons)–130.1–61.7=104.2 kcal/mol. The internal energy of the C_3H_2 is thus $104-E_T$, and this exceeds its bond dissociation energy for $E_T < 20.2$ kcal/mol. Since some translation energy is carried away by the first bond dissociation (see Fig. 1), lower values of E_T are allowed, consistent with the distribution in Fig. 4(c). For allene, the appropriate first and second C–H bond dissociation energies to form propargyl and propadienylidene are 87.4 and 102.5 kcal/mol, respectively, leading to C_3H_2 dissociation for $E_T < 22.1$ kcal/mol in the zero translational energy limit for the C_3H_3+H channel.

Branching ratios for the primary channels were obtained from TOF measurements on the EI instrument. The

$C_3H_3:C_3H_2$ branching ratio (for primary C_3H_2) is 56:44 for propyne dissociation and 64:36 for allene dissociation. About 8% and 9.7% of the C_3H_3 from propyne and allene, respectively, undergoes further dissociation to C_3H_2 . The allene results are quite different from the results obtained on a similar instrument by Jackson *et al.*,⁶ in which the reported branching ratio is 89:11. The likely source of this discrepancy is the overlapping contributions to the TOF spectra at mass 38 from processes (a) and (b), defined previously. Our measurements on the PI instrument enable us to characterize the primary $C_3H_2+H_2$ channel from allene very well, allowing us to better distinguish the two contributions to the EI TOF spectra than was possible previously.

In summary, we have studied the photodissociation of propyne and allene at 193 nm. Measurements using tunable VUV radiation to ionize the photoproducts enable unambiguous identification of the radical photoproducts. We find that the C_3H_3 products from C–H bond fission in propyne and allene are the propynyl and propargyl radicals, respectively, indicating highly bond-selective chemistry in propyne where the much stronger acetylenic C–H bond is preferentially dissociated. We also observe $C_3H_2+H_2$ as a significant primary channel for both reactants, and the VUV ionization measurements show this to be primarily the propadienylidene isomer

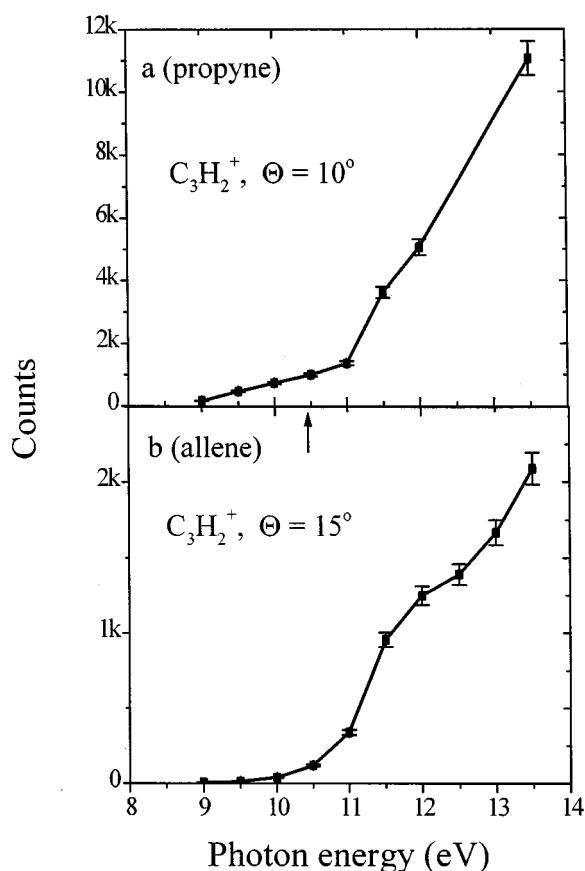


FIG. 5. Photoionization efficiency curves of C_3H_2 product from (a) propyne and (b) allene dissociation. Arrow along energy axis at 10.43 eV indicate ionization potential for propadienylidene from Table I.

in both cases. We expect that the combination of molecular beam scattering with VUV ionization detection will continue to be a powerful addition to the arsenal of experimental methods in reaction dynamics.

ACKNOWLEDGMENTS

This research is supported by the Director, Office of Basic Energy Sciences, Chemical Sciences Division, of the U.S. Department of Energy under Contract No. DE AC03-76SF00098.

- ¹J. A. Miller and C. F. Melius, *Combust. Flame* **91**, 21 (1992).
- ²M. S. Robinson, M. L. Polak, V. M. Bierbaum, C. H. DePuy, and W. C. Lineberger, *J. Am. Chem. Soc.* **117**, 6766 (1995).
- ³D. A. Ramsay and P. Thistlethwaite, *Can. J. Phys.* **44**, 1381 (1966).
- ⁴S. Satyapal and R. Bersohn, *J. Phys. Chem.* **95**, 8004 (1991).
- ⁵K. Seki and H. Okabe, *J. Phys. Chem.* **96**, 3345 (1992).
- ⁶W. M. Jackson, D. Anex, R. E. Continetti, B. A. Balko, and Y. T. Lee, *J. Chem. Phys.* **95**, 7327 (1991).
- ⁷Y. T. Lee, J. D. McDonald, P. R. LeBreton, and D. R. Herschbach, *Rev. Sci. Instrum.* **40**, 1402 (1969).
- ⁸A. M. Wodtke and Y. T. Lee, *J. Phys. Chem.* **89**, 4744 (1985).
- ⁹X. Zhao, Ph.D. thesis, University of California, Berkeley, 1989.
- ¹⁰X. Yang, J. Lin, Y. T. Lee, D. A. Blank, A. G. Suits, and A. M. Wodtke, *Rev. Sci. Instrum.* **68**, 3317 (1997).
- ¹¹H. M. Rosenstock, K. Draxl, B. W. Steiner, and J. T. Herron, *J. Phys. Chem. Ref. Data* **6**, 1 (1977).
- ¹²F. P. Lossing, *Can. J. Chem.* **50**, 3973 (1972).
- ¹³H. Clauberg, D. W. Minsek, and P. Chen, *J. Am. Chem. Soc.* **114**, 99 (1992).
- ¹⁴K. Yokoyama, unpublished results: Vertical ionization energies for propynyl were calculated by 11.0, 11.1, and 10.8 eV at three different levels of theory implemented in GAUSSIAN 94: B3LYP/6-31G, CCSD(T)/cc-pVTZ, and UOVGF/cc-pVTZ, respectively. The equilibrium geometry of the neutral ground state was optimized at the B3LYP/6-31G level (1998).
- ¹⁵X. Song, Y. Bao, R. S. Urdahl, J. U. Gosine, and W. M. Jackson, *Chem. Phys. Lett.* **217**, 216 (1993).
- ¹⁶L. Vereecken, K. Pierloot, and J. Perters, *J. Chem. Phys.* **108**, 1068 (1998).
- ¹⁷D. A. Blank, Ph.D. thesis, University of California, Berkeley, 1997.
- ¹⁸A. M. Mebel, W. M. Jackson, A. H. H. Chang, and S. H. Lin, *J. Am. Chem. Soc.* **120**, 5751 (1998).
- ¹⁹C. Ochsenfeld, R. I. Kaiser, Y. T. Lee, A. G. Suits, and M. Head-Gordon, *J. Chem. Phys.* **106**, 4141 (1997).